water

MDPI

Article

Recovering Nitrogen from Anaerobic Membrane Bioreactor Permeate Using a Natural Zeolite Ion Exchange Column

Jesús Godifredo, Laura Ruiz, Silvia Hernández, Joaquín Serralta and Ramón Barat *

CALAGUA—Unidad Mixta UV-UPV, Instituto de Ingeniería del Agua y Medio Ambiente, Universitat Politècnica de València, Camino de Vera s/n, 26022 Valencia, Spain
* Correspondence: rababa@dihma.upv.es

Abstract: In the framework of a circular economy, wastewater treatment should be oriented toward processes that allow the recovery of the resources present in the wastewater while ensuring good effluent quality. Nitrogen recovery is usually carried out in streams concentrated in this nutrient because these high concentrations facilitate nitrogen valorization. On the other hand, the mainstream of a wastewater treatment plant (WWTP) has a high potential for nitrogen recovery, but it is not usually considered because it is hard to manage due to its low nitrogen concentration. To solve this problem and facilitate the recovery of nitrogen in the mainstream, this work proposes ion exchange with zeolites as a stage of ammonium concentration, to provide a nitrogen-concentrated stream that could be valorized by another technology, while obtaining a nitrogen-free effluent. The working stream, the permeate of an AnMBR process in the mainstream, has suitable characteristics to be treated in an ion exchange column (free of suspended solids and with very low organic matter content). To this end, the effect of the working flow rate (17.5 to 4.4 BV/h) and the ammonium concentration (54 to 17 mg NH_4-N/L) on the adsorption capacity of the zeolite in the loading phase was evaluated. The adsorption curves were fitted to three mathematical models: Thomas, Bohart–Adams, and Yoon–Nelson. The effect of the regeneration flow rate (from 8.7 to 2.2 BV/h) and the regenerant concentration (NaOH at 0.2, 0.1, and 0.05 M) on regeneration capacity and efficiency were also studied. A novel control strategy based on effluent conductivity was used in both phases to control the duration of the adsorption and regeneration phases.

Keywords: AnMBR; nitrogen recovery; natural zeolite; ion exchange column

check for updates

Citation: Godifredo, J.; Ruiz, L.; Hernández, S.; Serralta, J.; Barat, R. Recovering Nitrogen from Anaerobic Membrane Bioreactor Permeate Using a Natural Zeolite Ion Exchange Column. *Water* **2024**, *16*, 2820. https://doi.org/10.3390/w16192820

Academic Editor: Andrea G. Capodaglio

Received: 27 August 2024
Revised: 28 September 2024
Accepted: 29 September 2024
Published: 4 October 2024

Copyright: © 2024 by the authors. Licensee MDPI, Basel, Switzerland. This article is an open access article distributed under the terms and conditions of the Creative Commons Attribution (CC BY) license (https://creativecommons.org/licenses/by/4.0/).

1. Introduction

The current climate situation and future perspectives point to water scarcity and climate change as two of the biggest challenges facing us today [1,2]. A new economic model based on the circular economy is therefore needed to allow the use of different sources of water, energy, and resources to address future scenarios [3]. This paradigm shift in the consumption of resources and waste generation has also extended to wastewater treatment plants (WWTPs), traditionally regarded as a set of simple pollution removal processes. However, this sector is now evolving toward the concept of water resource recovery facilities (WRRF). Filtration membrane technology has been proposed as a good alternative to the current processes and has been extended to multiple applications to improve energy production and resource recovery in water treatment facilities. Previous studies implemented this technology in microalgae treatment as membrane photobioreactors (MPBR) [4,5] or Direct Membrane Filtration (DMF) before the classical activated sludge process to enhance biogas production and nutrient recovery without the need for significant modification of already operating WWTPs [6]. Anaerobic membrane bioreactors (AnMBR) integrate in a single stage the retention of organic matter by means of filtration membranes together with its energy recovery by means of anaerobic digestion [7].

Filtration improves organic matter retention and biogas production in anaerobic digestion [8]. On the other hand, the permeate stream produced is free of suspended solids with hardly any organic matter but with nearly the same concentration of nutrients as the filtration influent [9,10]. In areas with no nitrogen and phosphorus discharge limits, this permeate can be directly discharged or used in fertigation, as long as the output TSS, COD, and microbiological characteristics comply with the established regulations. However, this stream must be treated when there is a nitrogen and phosphorus discharge requirement. In the case of nitrogen, due to its low COD/N ratio, as the conventional nitrification–denitrification process cannot be applied, new alternative methods must be studied [11].

Nitrogen recovery appears as a feasible option in this scenario, with a stream free of suspended solids, low organic matter concentrations, and a similar ammonium concentration to that in the influent. Hollow Fiber Membrane Contactors (HFMCs) appear as a promising technology for N recovery [12]. However, for this technology to be technically and economically feasible, high concentrations of nitrogen in its ammoniacal form are needed [13]. This technology has been mainly used for high N concentration streams, such as the supernatant of digested sludge [12] with high ammonium concentrations. In order to apply HFMC to the AnMBR permeate, the nitrogen must be concentrated, with ion exchange being a promising alternative as there are no solids and hardly any organic matter in the permeate [14].

The ion exchange process has two phases: adsorption and regeneration. In the adsorption phase, the cation exchange column retains NH_4^+ until its active points are saturated and NH_4^+ can be detected in the effluent. The time to reach the breakpoint depends on various factors such as temperature, pH, working flow, or inlet ammonium concentration [14–16]. The column must be regenerated when the ammonium setpoint value in the effluent is reached, and in this phase, the retained ammonium is displaced by another cation. Due to the degree of affinity, either NaCl [17,18] or NaOH [19] is normally used, although other compounds such as KCl [20] can also be considered.

During regeneration, the main objective is to return the column to its initial state without losing efficiency for the next adsorption cycle, while generating a highly concentrated ammonium current. It is usually possible to concentrate between 8 and 20 times the influent ammonium, although this value is determined by the working variables such as the chosen regenerant and its concentration and the regeneration flow [14].

Two types of materials are mainly used for cation exchange: zeolites and cationic resins, the latter having a greater capacity to retain ammonium. However, although zeolites offer a slightly lower exchange capacity, they have a greater affinity and selectivity for ammonium [15,20]. Some studies [21,22] have demonstrated the potential of clinoptilolite as an effective adsorbent to remove and recover ammonia from real AnMBR permeate. Moreover, recently, ref. [23,24] studied the combination of zeolites as a sorption stage and HFMC for ammonia recovery to WWTP effluent (mainstream, 50 mg N-NH_4/L) and anaerobic digestion supernatant (sidestream, 600–800 mg N-NH_4/L).

However, the application of zeolites at full scale still faces some challenges [25]. A key factor to consider in order to reduce the size and operating time is automated control during the adsorption and regeneration phases. This includes modeling N-NH_4 breakthrough curves [26], finding correlations with parameters that can be measured online to detect these breakthrough curves, and studying the effect of factors such as flow rate, initial concentration, and particle diameter. The flow rate during saturation has been studied by many authors such as [27], but regarding the development of a mechanism to control the duration of the adsorption and regeneration phases and thus optimize the working time of the columns, it is hard to find references.

Many studies have been carried out on synthetic waters that do not consider the strong influence of the wastewater components on the behavior of the adsorbent material [20], and there is no mechanism to control the duration of the adsorption and regeneration phases to optimize the working time of the columns. The recovery of nitrogen and other nutrients is

usually handled in concentrated streams, like digestion supernatants. This study, however, focuses on recovering ammonium from the mainstream flow. Although this flow has significant potential, it is difficult to manage due to its low nitrogen concentration. To overcome this, a concentration process using zeolites is applied to produce a stream with a more suitable ammonium concentration for further recovery methods, such as membrane contactors. In addition, another novelty of the process is that the stream to be treated comes from the permeate of an AnMBR process. The general objective of this study was thus to optimize the zeolite ion exchange performance during the saturation and regeneration phases. For this, the influence of the working flow rate and the input concentration of ammonium on the cation exchange capacity of a zeolite exchange column in its sodium form (clinoptilolite) was determined. Based on the experimental data, bibliographic models were adjusted to determine the evolution of each adsorption curve, the minimum height of the bed, and the average time for which the column had been saturated to 50%. The effect of the variables studied on the model parameters was also analyzed. For regeneration, the regenerant concentration and working flow that achieved the highest ammonium concentration factor were identified, while effluent conductivity was used as a soft sensor measure to determine the breakpoint and end of the regeneration phase.

2. Materials and Methods

2.1. Materials

Adsorption and regeneration tests were carried out on a column with an internal diameter of 4 cm and a height of 20 cm. A peristaltic pump (LLG-uniPeristalticPUMP 3) was used to pump bottom-up either the working water or the regenerating solution. The characteristics of the column are shown in Table 1. The column was filled with zeolite clinoptilolite from Zeocem with a particle size of 0.5–1.0 mm and was pre-activated with NaOH 1 M for a one-hour contact time. Further information on the characterization of this adsorbent material can be found in Godifredo et al. (2023) [28]. The zeolite contains 74.2%wt of SiO_2 and 12.20%wt of Al_2O_3, so the Si/Al molar ratio is over 5 (detailed chemical and structural characterization can be found in [29]). A diagram of the setup is shown in Figure 1.

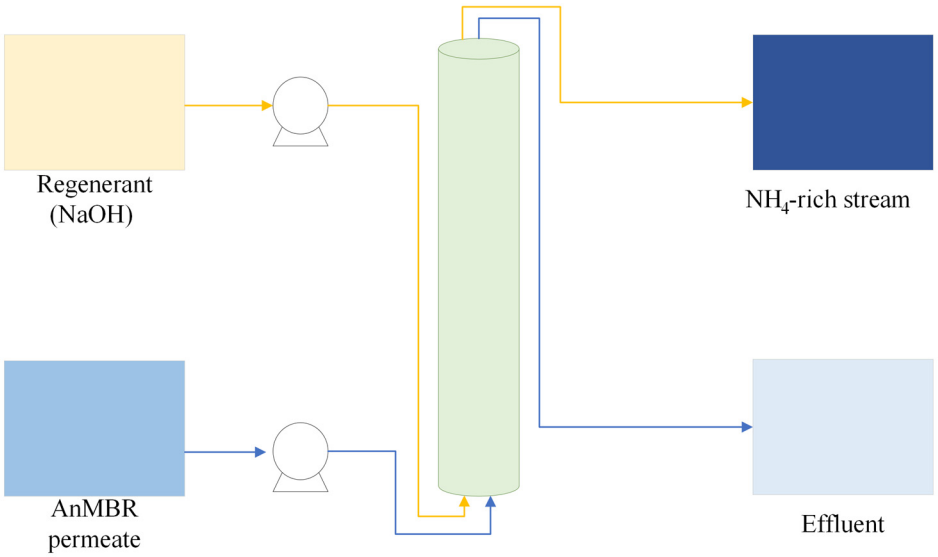

Figure 1. Diagram of the setup. The streams in blue represent the load phase, while the streams in yellow indicate the regeneration phase.

Table 1. Characteristics of the ion exchange column.

Parameter	Value
Height	20 cm
Diameter	4 cm
Zeolite dry mass	217 g
Empty volume	250 mL
Porosity	0.44
Bed volume (BV)	111 mL

All the tests were performed on permeate obtained from an AnMBR using a PULSION® Koch Membrane Systems commercial membrane module with a pore size of 0.03 µm and 43.5 m^2. The water had been previously sieved and homogenized. The pilot plant was placed at the *Cuenca del Carraixet* WWTP (Valencia, Spain).

The permeate was fortified with NH_4Cl for the experiments when required, while in those with a lower ammonia concentration, the permeate was diluted with tap water to maintain the concentration of the remaining cations (tap water cation concentration was similar to that of permeate [28]). The permeate had a concentration of 27 mg NH_4-N/L, was free of suspended solids, had a pH of 7.3, and contained little organic matter (70 mg COD/L and 17 mg BDO/L) (Table 2).

Table 2. Permeate characterization.

Parameter	Value
COD (mg COD/L)	73 ± 19
BOD (mg BOD/L)	17 ± 6
NH_4 (mg NH_4-N/L)	27.2 ± 8.8
Ca^{2+} (mg Ca^{2+}/L)	119.0 ± 15.1
Mg^{2+} (mg Mg^{2+}/L)	32.3 ± 5.1
Na^+ (mg Na^+/L)	109 ± 7.6
K^+ (mg K^+/L)	14.4 ± 2.0
PO_4^{3-} (mg PO_4^{3-}-P/L)	3.9 ± 1.2
pH	7.4 ± 0.6
Alkalinity (mg $CaCO_3$/L)	345 ± 116

2.2. Adsorption Test

The effect of the ammonium concentration on the influent, as well as the working Empty Bed contact time (EBCT), were evaluated in a set of 9 trials resulting from the combination of 3 values for each of these two variables. The central value of the ammonium concentration was that of its concentration in the AnMBR permeate (27 mg NH_4-N/L). Double and half of this concentration were also selected. For EBCT optimization, a starting value of 6.9 min was established (following the working values of other authors such as [16,19,22], and similarly to the ammonium concentration, its double and half values were also selected. Table 3 shows the set of experiments carried out combining EBCT and NH_4 concentrations. To compare the adsorption capacity value (q_{ads}) of the conditions studied in the saturation column experiments, a set point of 0.5 mg NH_4-N/L in the column effluent was established, and the experiment was ended when the column effluent reached the set point.

Large amounts of permeate were stored to keep the working water matrix as homogeneous as possible between experiments. Alyltiurea was added as the nitrification inhibitor, since it had been found that some of the ammonium in the collected permeate was oxidized to NOx during storage. When this inhibitor was added, no change was found in the NH_4 concentration.

Table 3. Column adsorption tests.

Test	EBCT (min)	BV/h	C_O (mg NH_4-N/L)
A1	3.4	17.5	14
A2	6.9	8.7	14
A3	13.8	4.4	14
A4	3.4	17.5	27
A5	6.9	8.7	27
A6	13.8	4.4	27
A7	3.4	17.5	54
A8	6.9	8.7	54
A9	13.8	4.4	54

The ammonium adsorption capacity in individual tests was calculated according to the following equation (Equation (1)):

$$q_{ads} = \frac{\int_0^{V_t} (C_0 - C) dVt}{m} \quad (1)$$

where q_{ads} is the ammonium adsorption capacity at the volume V_t (mg NH_4-N/g), V_t is the volume of permeate treated at time t, C_0 and C are the concentrations of ammonium in the influent and effluent at volume V_t, respectively (mg NH_4-N/L), and m is the zeolite mass (g).

2.3. Adsorption Models

After the 9 experimental tests at different Co and Q and the rupture curves obtained, a set of mathematical models was applied to describe the behavior. Three kinetic models were selected from the literature: the Thomas model, the Bohart–Adams model, and the Yoon–Nelson model.

The Thomas model, one of the most widely used general models to represent the behavior of the ion exchange column [30], was developed in 1944. This model shows a good fit if the isotherm test has a close correlation to the Langmuir model. The Thomas model assumes that there is no axial dispersion and that adsorption is reversible and follows second-order kinetics [31]. This model is used to obtain the rupture curve of the column and the maximum adsorption capacity. The linearized Thomas model can be explained by Equation (2):

$$ln\left(\frac{C_0}{C_t} - 1\right) = \frac{k_{th} \cdot q_{0(th)} \cdot m}{Q} - \frac{k_{th} \cdot C_0}{Q} \cdot V_t \quad (2)$$

where C_o is the influent concentration (mg NH_4-N/L), C_t is the concentration of the effluent at time t (mg NH_4-N/L), m is the adsorbent mass (g), kth is the Thomas constant (mL/min *mg), $q_{0(th)}$ is the maximum adsorption capacity at equilibrium (mg/g), Q is the treatment flow rate (mL/min), and V_t is the volume treated at time t. From the linear representation of $ln\left(\frac{C_0}{C_t} - 1\right)$ vs. V, the values of k_{th} and $q_{0(th)}$ can be obtained.

The Bohart–Adams model assumes that the adsorption rate is proportional to the residual adsorption capacity of the adsorbent and the concentration of the adsorbate [32]. Its general equation is developed in Equation (3).

$$ln\left(\frac{C_O}{C_t} - 1\right) = ln\left(e^{\frac{k_{BA} \cdot q_{BA} \cdot H}{v}} - 1\right) - k_{BA} \cdot C_O \cdot t \quad (3)$$

where K_{BA} is the Bohart–Adams constant (L/mg min), H is the height of the column bed (cm), v is the linear velocity of the flow (cm/min), t is the time (min), and q_{BA} is the maximum adsorption capacity at equilibrium by the Bohart–Adams model (mg/g). However, because the term exponential is usually much greater than 1 and is mainly used

to describe the initial part of the breakdown curve (Ct < 0.15 C_0), the equation can be simplified to the following expression in Equation (4).

$$ln\left(\frac{C_O}{C_t}\right) = k_{BA} \cdot C_O \cdot t - k_{BA} \cdot q_{BA} \cdot \frac{H}{v} \quad (4)$$

The model parameters can be obtained through the linear representation of $ln\left(\frac{C_O}{C_t}\right)$ vs. t. Once this model is adjusted, it is possible to calculate the minimum bed height required (Z_o, in cm) so that the effluent concentration is equal to C_b for t = 0 using the formula, where Cb is the set point for the ammonium concentration in the effluent (0.5 mg N-NH_4/L for this study), as shown in Equation (5):

$$Z_0 = \frac{v}{k_{BA} \cdot q_{BA}} \cdot ln\left(\frac{C_0}{C_b} - 1\right) \quad (5)$$

The Yoon–Nelson model is a simple model that needs less experimental data for calibration and less information on the adsorbate characteristics, adsorbent type, and physical properties of the bed [33]. This model can predict the time at which 50% of the maximum adsorption capacity will be reached. The equation for this model is given in Equation (6):

$$ln\left(\frac{C_t}{C_0 - C_t}\right) = k_{YN} \cdot (t - \tau) \quad (6)$$

where k_{YN} is the Yoon–Nelson constant (min^{-1}), and τ is the time at which 50% of the column saturation (min) is reached.

The ability of these models to fit the experimental data was evaluated by calculating the mean root mean squared error (RMSE) using Equation (7):

$$RMSE = \sqrt[2]{\frac{1}{N-2}\sum_{i=1}^{N}\left(q_{exp,i} - q_{eth,i}\right)^2} \quad (7)$$

where N is the sample size, $q_{exp,i}$ is the experimental value of q_e for sample i, and $q_{eth,i}$ is the value of q_e obtained using the model under the same conditions as $q_{exp,i}$.

2.4. Regeneration Test

Regeneration tests were carried out in 5 experiments. The first three were conducted at the same EBCT (27.5 min) at which the concentration of NaOH (0.05, 0.1, and 0.2 M) was studied. The influence of the regeneration flow was studied at the NaOH concentration selected after the first group of tests (see Table 4). To avoid the effect of other variables on the results, such as the amount of ammonium retained, the columns were all saturated under the same conditions: a flow of 17.5 BV/h (the highest flow rate studied with an adequate contact time) and ammonium concentration of 20.8 mg NH_4-N/L (the permeate concentration during the regeneration experiments).

Table 4. Regeneration test.

Test	EBCT (min)	BV/h	NaOH (M)
R1	27.5	2.2	0.05
R2	27.5	2.2	0.1
R3	27.5	2.2	0.2
R4	13.9	4.3	0.1
R5	6.9	8.7	0.1

As in the adsorption test, an experiment was carried out to determine the relationship between conductivity and ammonium release.

2.5. Conductivity Monitoring Tests

To evaluate the possible relationship between conductivity and effluent ammonium concentration during the adsorption and regeneration phases, two additional tests were carried out. For the adsorption phase test, an influent ammonium concentration of Co = 18 mg NH_4-N/g and a working flow rate Q = 17.5 BV/h were established. For the regeneration phase, the working flow rate was maintained at 17.5, and the NaOH concentration used was 0.1 M. In both cases, frequent samples were taken to monitor conductivity, ammonium, and other cations, especially Na^+, since it is the most exchanged cation in NH_4^+ adsorption.

3. Results

3.1. Adsorption Test

3.1.1. Effect of Treatment Flow

Analyzing the results obtained in Figure 2, it can be seen that a longer contact time improves the adsorption capacity of the zeolite. The change in the flow rate from 17.5 BV/h to 4.4 BV/h raised the adsorption capacity to 35% (Co = 27 and 54 mg NH_4-N/L). As the zeolite becomes saturated in ammonium, the gradient between ammonium permeate and the ammonium adsorbed on the zeolite decreases along with the rate of exchange. Most authors have detected similar ammonium adsorption to the one obtained in the present study (Table 5). This behavior is not exclusive to natural zeolites as an adsorbent or ammonium, since ref. [34] recorded a 35% reduction in the ability to adsorb ammonium of a strong cationic resin when going from a flow rate of 8 to 24 BV/h and ref. [24] found an 11% reduction when multiplying the working flow by 3, working on a column filled with a graphene oxide aerogel to retain Cr(VI) from water.

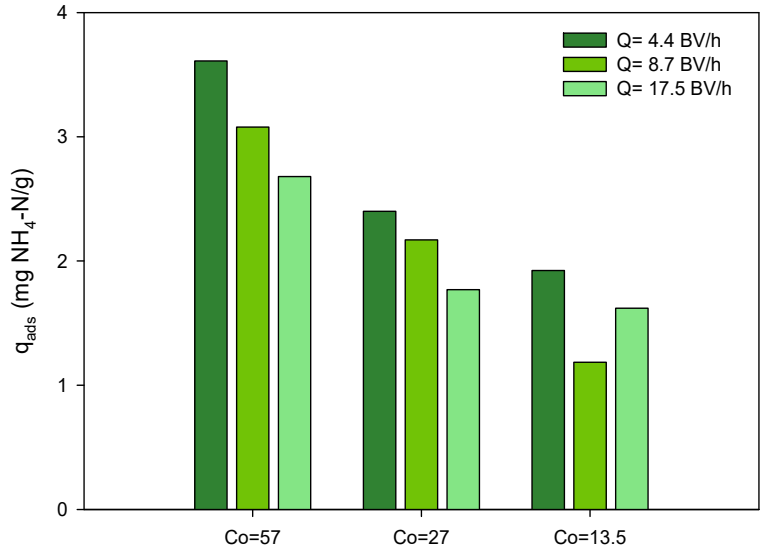

Figure 2. Ammonium adsorption capacity according to the working flow rate.

Table 5. Improvement in ammonium adsorption capacity when the working flow rate is reduced.

Test	Baseline Flow Rate (BV/h)	Final Flow Rate (BV/h)	Improvement in Ammonium Adsorption Capacity (%)
This study	17.5	4.4	35%
[35]	31.2	17.1	100%
[36]	39.0	26.0	30%
	39.0	7.7	120%
[37]	15.0	5.0	10%
[22]	8.0	4.0	10%
[27]	24.0	8.0	50%

3.1.2. Effect of Ammonium Concentration on the Influent

The concentration of ammonium in the influent had an effect similar to that found in the literature, since the higher the ammonium concentration in the water to be treated, the higher the adsorption. Regarding the adsorption capacity, when the ammonium concentration increased from 27 to 54 mg NH_4-N/L, the adsorption capacity dropped to around 50% for all the working flows studied, while when the influent concentration was reduced to 14 mg NH_4-N/L, the adsorption capacity was reduced from 90% to 50% (depending on the working flow rate) compared to the value obtained with Co = 27 mg NH_4-N/L.

In this regard, ref. [38] found a reduction in q_{ads} from 22 to 17.9 mg/g when the incoming ammonium concentration was reduced from 80 to 30 mg NH_4-N/L. Ref. [39] reported similar behavior when the input concentration was increased 2.5 times and obtained 1.8 times the adsorption capacity. This is mainly because the higher the ammonium in the fluid, the greater the gradient with respect to the initial zeolite concentration when the zeolite has not yet retained ammonium. A higher concentration gradient between the zeolite and the medium allows a greater exchange of ammonia [40]. Although the concentration of ammonium in the influent is not an operational parameter to be modified, it is necessary to take it into account since real water presents variations in its quality over time.

The adsorption capacity data obtained are similar to those recorded by other authors in adsorption column assays using real water (Table 6). As found in ref. [16], the presence of calcium and other components (such as Mg^{2+}) has a great impact on the adsorption capacity obtained experimentally. On the other hand, the influence of the initial ammonium concentration could be observed in ref. [40], since by working with Co = 600 mg NH_4-N/L, they were able to obtain ammonium adsorption capacities between 27 and 36 mg NH_4-N/g. As in the results obtained by Godifredo et al. (2023) [28], the type of influent being worked with must be considered, and then the results must be compared under similar conditions.

Table 6. Comparison of the results obtained with other authors.

Reference	Material	C_o (mg NH_4-N/L)	Q (BV/h)	q_{ads} (mg NH_4-N/g)
This study	Clinoptilolite-Na	54	4.4	3.61
[41]	MesoLite	20		5.0
[20]	Zeolite-N (Nanochem)	8	6	3.9
[22]	Clinoptilolite	31	4–8	3.1–2.9
[35]	Clinoptilolite	40	17	8.0
	Purolite C104	40	50.6	5.7
[40]	MesoLite	600	5	27–36
[24]	Clinoptilolite-Na	66	10	5.1
[16]	Natural zeolite	25	4	6.61 (without Ca^{2+})
				4.48 (60 mg Ca^{2+}/L)
			6	5.71 (without Ca^{2+})
				4.00 (60 mg Ca^{2+}/L)
			12	4.05 (without Ca^{2+})
				2.85 (60 mg Ca^{2+}/L
[42]	Natural zeolite	30	4	3.01

3.1.3. Adsorption Phase Conductivity

Conductivity behavior was monitored to find a relationship with the influent ammonium concentration to establish possible patterns to control the adsorption phase. Since every ion has a different conductance value, the evolution of this value can detect changes in the variation of the ions involved in the process and provide a better understanding of the process with simple soft sensor measures. The breakpoint was therefore identified through changes in the conductivity trend.

Variation between the input and output conductivity of the process thus depends on the cations involved in the adsorption process and their role (whether adsorbed or replaced) [43]. Since the molar conductivity of the main cations involved in ion exchange at 25° is 50.1 S·cm^2/mol for Na^+, 73.5 for NH_4^+, and 106.0 for Ca^{2+} [44], a reduction of

23.4 S cm^2/mol should be found each time 1 meq/L of NH_4^+ is exchanged for Na^+, at 25 °C of working temperature.

Analyzing the conductivity and ammonium (Figure 3), an initial drop in conductivity can be seen, followed by a stage in which this value increases. Zeolites are initially activated in their Na form, so in the early stages, a large amount of Na is released as NH_4^+ is retained (Figure 3), causing a decreasing tendency in conductivity. When the column is saturated and the breakpoint is reached, the variation in the conductivity trend changes, increasing due to the ammonium excess in the column effluent. These variations can be used to monitor the process performance to maintain the nitrogen effluent concentrations below the legal requirements. Other authors, such as ref. [35], also found the breakpoint of ammonium using a strong acidic cationic resin. In these cases, they also detected that the breakpoint of the column was associated with the moment at which the effluent conductivity begins to tend toward the input conductivity values.

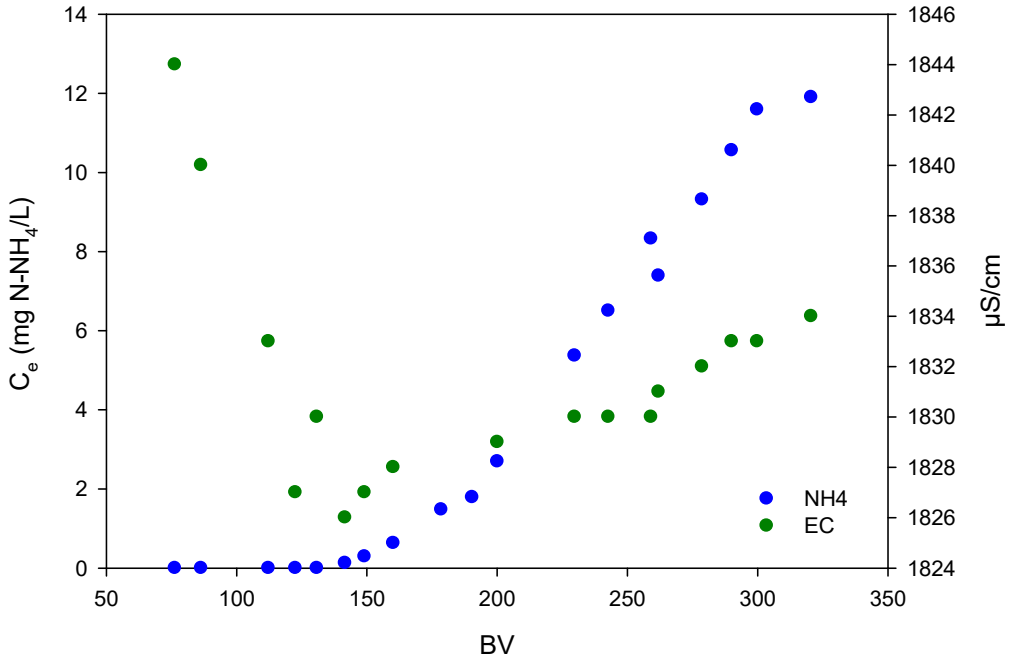

Figure 3. Evolution of ammonium and conductivity during the adsorption phase after 70 BV.

3.2. Regeneration Test

NaOH was used as the regenerant for the regeneration study of the exchange column, since NaOH provides Na to replace the adsorbed NH_4^+ and displaces the working pH toward basic values that favor the release of ammonium [45]. The high pH of the concentrated ammonium stream facilitates the integration of cation exchange with HFMC to recover ammonium as a fertilizer. When NaCl is used, the concentrations necessary for regeneration are higher; ref. [17] worked with 30 g/L of NaCl and ref. [46] at 58.44 g/L. When NaOH is used as a reagent, the concentrations are lower. Ref. [40] used 5 g/L, ref. [19] used 2 g/L, and in the present study, a range from 2 to 8 g/L of NaOH was employed. Although some authors have used another type of cation to displace NH_4^+, such as KCl [20], this paper has worked with NaOH, taking into account the Na+ and NH_4 selectivity of the working zeolite.

Initially, the effect of the NaOH concentration was studied for a flow rate of 2.2 BV/h, having saturated the columns under the same conditions (Co = 20.8 mg NH_4-N/L and Q = 17.5 BV/h). The results show that as the concentration of the regenerator increases, less volume is needed to recover the column (Figure 4), and therefore a more concentrated current can be obtained, reaching a current concentration of 765 mg NH_4-N/L for NaOH = 0.2 M (Figure 5). However, when calculating the amount of NH_4-N recovered per gram of Na^+ in the regenerant stream, it is concluded that the 0.1 M concentration could ex-

tract more NH_4 for each gram of Na^+ in the regeneration solution, yielding 0.221 mg NH_4-N replaced/mg Na added (Figure 5). At this NaOH concentration, a concentrated ammonium stream of 615 mg NH_4-N/L was obtained (Figure 5), indicating a more efficient use of the regenerant than those obtained by other authors. Ref. [35] obtained 0.047 mg NH_4-N/mg Na using NaCl at 30 g/L as regenerant, ref. [40] obtained 0.002 mg NH_4-N/mg Na using 58.5 g/L of NaCl to regenerate, and ref. [39] obtained 0.0018 mg NH_4-N/mg Na while working with 175 g/L of NaCl. Based on these good results and the ability to concentrate ammonium up to 30 times with respect to the input concentration, a concentration of 0.1 M has been selected.

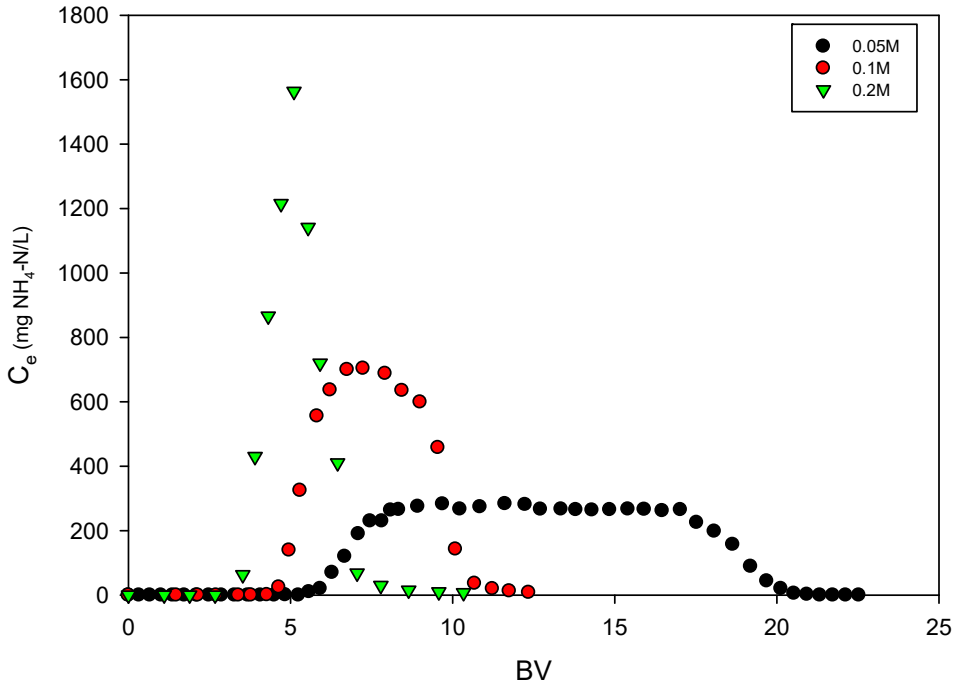

Figure 4. Evolution of ammonium in the effluent during regeneration at different concentrations of NaOH.

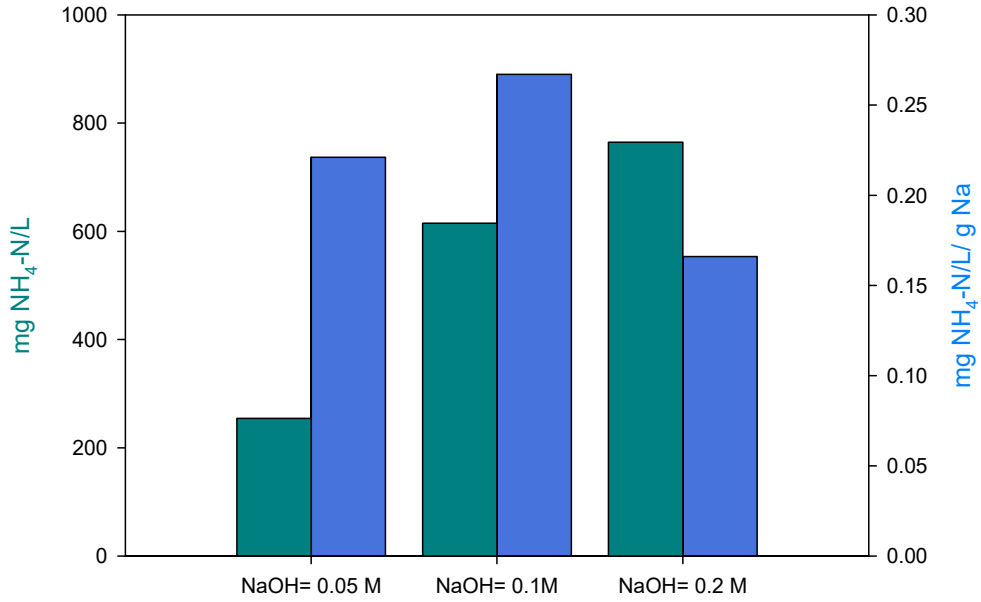

Figure 5. Ammonium concentration achieved and efficacy in the use of the regenerator at different concentrations of NaOH.

Once the concentration of the regenerant was selected, the influence of the regeneration flow on the final concentration obtained and the efficiency in the use of the regenerant was studied. Three trials were carried out at different working flows, but no significant differences were found between them (Figure 6). While in the loading tests, it has been seen how the flow rate influences the ammonium retention capacity, in the regeneration for the flow rates studied, there was no change in the ammonium recovery yields. A possible explanation is the mechanisms that govern cation exchange in the adsorbent. One of these mechanisms is the transfer of matter between the aqueous solution and the adsorbent, but due to the high concentration of Na^+ in the aqueous medium, the gradient between both phases is high, so the matter transfer rate is also high; thus, the working flow rate is not a limiting aspect in performance (within the range of the working flows studied), and the exchange rate is controlled by internal aspects of the adsorbent rather than by the operating parameters Ref. [47] obtained different results that are consistent with the proposed theory. As they worked with high concentrations of ammonium in the influent (500–1000 mg NH_4-N/L) while the concentration of regenerant was not equally high (Na_2CO_3 = 0.5 M), they did see that the regeneration flow caused changes in yields, obtaining an output concentration of 10,000 mg NH_4-N/L for Q = 0.5 BV/h, while when the flow rate was raised to 1.5 BV/h, the concentration was 4000 mg NH_4-N/L. This may be because the amount of Na supplied was not high enough to displace the NH_4^+ cations immediately, meaning that the contact time between the regenerator and the adsorbent is an aspect to be taken into account, as it can change the concentration in the recovery stream.

Given that no differences were found among the three study flows, the highest working flow (8.7 BV/h) was chosen, since it reduced the regeneration time in the column without a loss in performance.

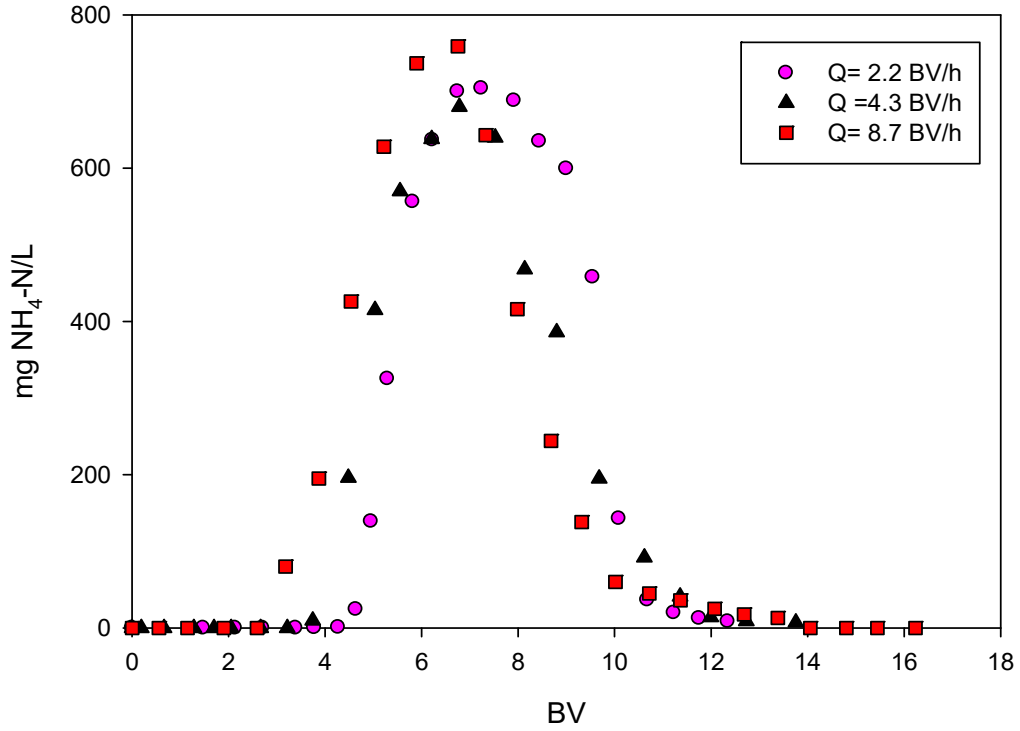

Figure 6. Evolution of ammonium in the effluent during regeneration at NaOH 0.1 M and different flow rates.

3.3. Conductivity in the Regeneration Phase

The relationship of conductivity with ammonium and sodium during the regeneration phase was also studied. In this case, the objective was to detect the end of ammonium release. The influent ammonium concentration (19 mg NH_4-N/L) was selected as a set

point to detect the end of the regeneration phase. Since the two main ions exchanged are sodium and ammonium, the same theoretical bases as those previously used in relation to the difference in molar conductivity can be applied.

In this case, the dependence of the conductivity on the Na+ content of the stream is even stronger (Figure 7). Because this cation is in a higher influent concentration (2300 mg Na/L) than the other predominant cation (ammonium 852 mg NH_4-N/L at the time of maximum concentration), it is expected that the variation in conductivity is governed by the variation of sodium in the effluent. In the first stage (up to 7 BV treated), the Na concentration is practically zero because all the sodium feed is undergoing cation exchange processes (transfer between liquid-solids, diffusion within the zeolite, and finally displacement of NH_4^+). During this period, sodium regenerates the column, and conductivity is correlated with NH_4 changes in the effluent, as shown in Figure 7. These slight changes are masked by the large variation caused by the later high concentration of sodium. If only the first 8 BV are considered (Figure S1), it can be clearly seen that there is a slight increase in conductivity as ammonium is collected in the effluent. After this slight rise, the variation rate increases because the excess Na^+ starts to appear in the effluent, so the variation in conductivity is clearly correlated with Na^+. Sodium concentration starts to increase in the effluent as the column regenerates. When all the ammonium has been released, conductivity tends toward the value of the regenerant stream (21.7 mS/cm).

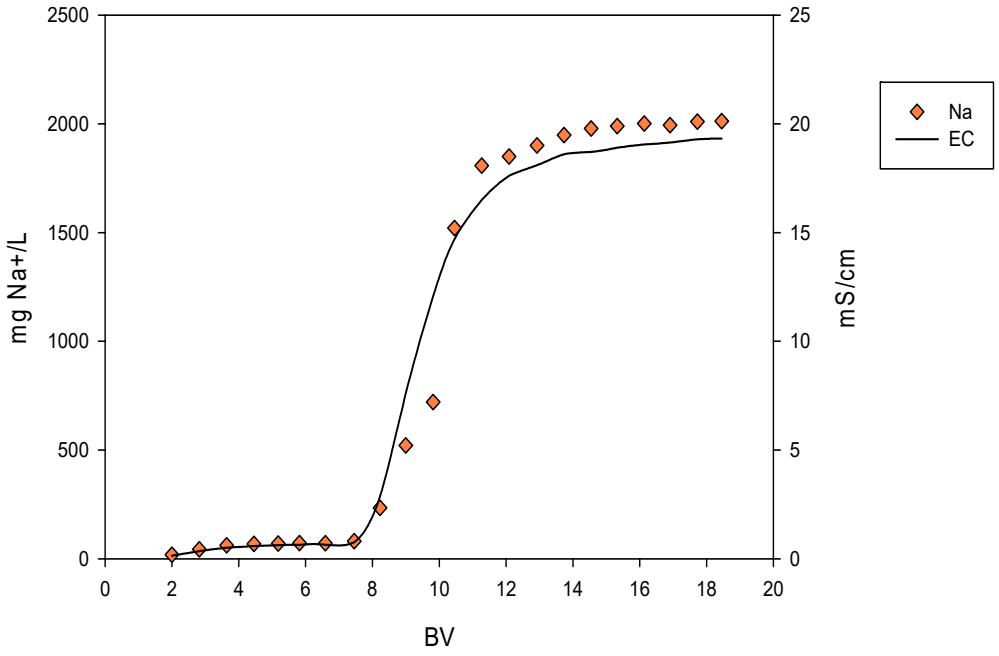

Figure 7. Evolution of sodium and conductivity during the regeneration phase.

The results obtained thus showed that when sodium is not being retained, it is because it has no ammonium to exchange; therefore, the time at which the regeneration phase ends is related to conductivity. Figure 8 shows the complete evolution of conductivity and ammonium. This graph shows that when the ammonium concentration reaches values close to zero, conductivity begins to stabilize around the influent value. Calculating the conductivity variation rate, the end of the regeneration phase can be determined. Figure 9 shows the evolution of ammonium in the effluent compared with the conductivity variation rate calculated at intervals of 100 s. After the sudden appearance of Na^+, the conductivity curve takes its highest value and subsequently slows down. When there is almost no ammonium left to exchange, the curve value is close to zero and remains constant. By identifying this change in conductivity, the duration of the regeneration phase can be adjusted and reduced.

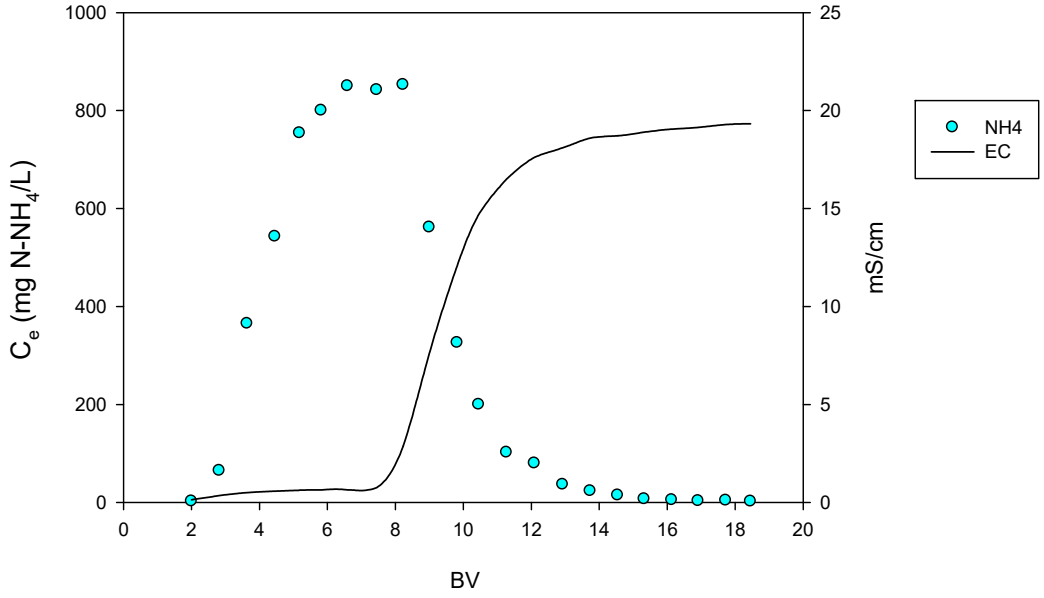

Figure 8. Evolution of ammonium and conductivity during the regeneration phase.

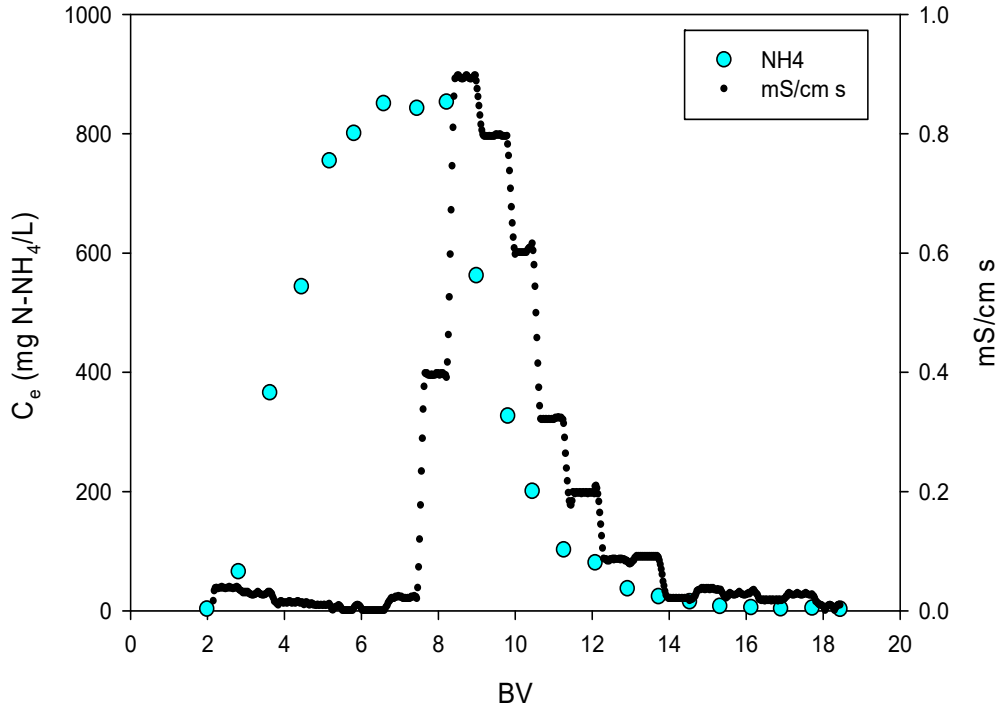

Figure 9. Evolution of ammonium and conductivity variation during the regeneration phase.

3.4. Model Fitting

3.4.1. Thomas

To calibrate the Thomas model, $ln\left(\frac{C_0}{C_t}-1\right)$ vs. V must be represented. The values of k_{th} and $q_{0(th)}$ are obtained by regression adjustment. Figure S2 shows some adjustments of the data obtained (R2 values higher than 0.97).

After the linear fit, the variables k_{th} and $q_{0(th)}$ as well as the RMSE of each test were calculated. Figure 10 and Figure S3 show the experimental data and those obtained from the Thomas model for tests 4 and 7. Table 7 summarizes the values obtained after model adjustment.

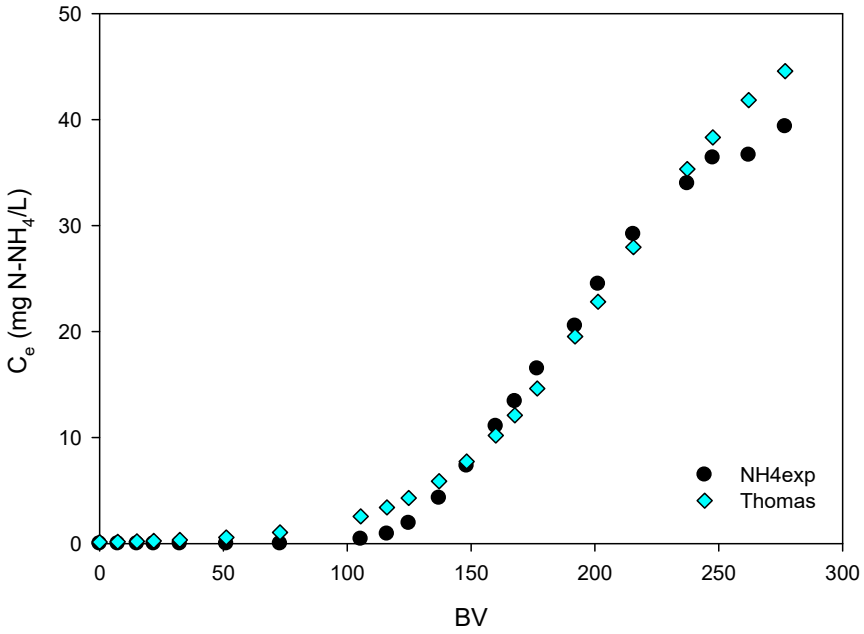

Figure 10. Fitting experimental data from the A4 trial using the Thomas model.

Table 7. Fit parameters for the Thomas model.

Test	Q (BV/h)	C_o (mg NH_4-N/l)	k_{th}	$q_{0(th)}$	RMSE
A1	17.5	12.5	0.049	2.180	0.080
A2	8.7	12.5	0.020	2.251	0.021
A3	4.4	12.5	0.017	2.411	0.025
A4	17.5	27	0.022	3.137	0.637
A5	8.7	27	0.014	3.318	0.719
A6	4.4	27	0.015	2.883	0.125
A7	17.5	54	0.009	5.490	2.103
A8	8.7	54	0.007	5.708	2.352
A9	4.4	54	0.005	5.843	0.508

The Thomas model correctly represents the experimental data obtained in the adsorption tests. Based on the mechanisms included in this model, it can be said that the internal and external diffusion resistances are not the limiting mechanisms in adsorption [33]. As can be seen in the adjustment data (Table 7), the theoretical maximum adsorption capacity ($q_{0(th)}$) increases with the concentration of ammonium in the influent and decreases with increasing working flow (q0(th) = 5.708, 3.137, and 2.251 mg NH_4-N/g for Q = 8.7 BV/h and Co = 54, 27, and 12.5 mg NH_4-N/L, respectively) (Figures S4 and S5). Similar behavior in this model parameter was also found by others [40,47]. These authors highlighted the idea that the transfer of matter governs the process, since the higher the concentration gradient between the aqueous and solid phases, the greater the exchange rate. However, as these differences are mostly observed at low ammonium concentrations [38], this mechanism is especially important when working with urban wastewater, as small changes in input quality will have a large impact on zeolite capacity.

The Thomas constant (Kth) shows the opposite behavior to the theoretical maximum capacity, since the higher the concentration of ammonium at the input, the lower the Kth value. As the working flow rate increases, so does the value of this parameter. This may be due to the fact that the higher the flow rate, the greater the turbulence generated at the solid-liquid interface, and therefore the transfer rate is higher. A similar trend was observed by others [33,47]. Ref. [42] obtained a Kth of 0.008 mL/mg min for Co = 5 mg NH_4-N/L and a value of 0.003 mL/mg min when C_0 = 30.5 mg NH_4-N/L.

Since the Thomas model can reproduce the rupture curve of the column, it is possible to know the time or volume treated by the column until a setpoint value is reached for specific working conditions. Table 8 shows the adsorption capacity of the zeolite before saturation and the amount of BV that the zeolite can treat until the ammonium in the effluent is higher than the set point (0.5, 10, and 15 mg NH_4-N/L). The greatest differences in the treatment capacity of the column as a function of the flow occur when the discharge requirements are highly restrictive. When the setpoint in the effluent is higher, the volume of permeate that can be treated is almost the same as when the working flow rate increases and the zeolite performance is more uniform. In Figure 11 (for C_o = 27 NH_4-N/L), it can be seen that the differences in the treatment flow, for the same concentration of ammonium in the influent, are reduced as the column approaches complete saturation.

This means that when designing and selecting the operating parameters of the column, it is important to know the discharge requirements that will be applied. If the maximum allowable output concentration is very low, the most suitable solution could be to apply a low treatment flow for better use of the zeolite exchange capacity at the cost of increasing the size of the column. However, when the discharge requirements are more flexible, a higher treatment flow rate can be used; although this entails a slight loss of zeolite efficiency, it significantly reduces the column EBCT and therefore its design size.

Table 8. BV and qads treated in each test and for each setpoint. Values were obtained by applying the calibrated Thomas model.

Test	0.5 mg NH_4-N/L		10 mg NH_4-N/L		15 mg NH_4-N/L	
	q_{ads}	BV	q_{ads}	BV	q_{ads}	BV
A1	1.62	261	2.15	380		
A2	1.55	227	2.19	402	Co > Ceff	
A3	2.08	321	2.38	415		
A4	1.38	103	2.74	220	2.91	243
A5	2.10	152	3.02	231	3.14	246
A6	2.30	176	3.11	249	3.23	265
A7	1.30	51	4.05	160	4.49	150
A8	2.78	83	4.69	165	4.89	175
A9	3.62	126	5.04	179	5.25	186

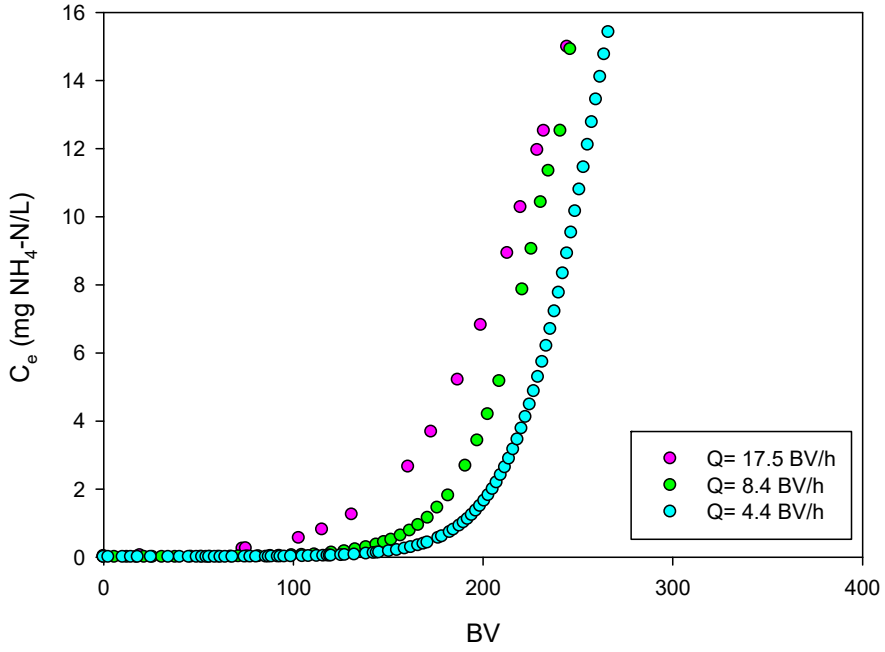

Figure 11. Evolution of ammonium in the effluent for different working flows and C0 = 27 mg NH_4-N/L.

3.4.2. Bohart–Adams

As previously explained, in the adjustment of this model, only ammonium concentration values less than 15% Co were used to perform the linear adjustment. These data show a good linear fit, as can be seen in the graphs in the Supplementary Material (Figure S6).

Figure S7 shows the fit of the experimental data with the concentration calculated by the Bohart–Adams model for trial A7. It can be seen how the model can reproduce what happens at the initial moments of the curve. However, as the column saturation increases, the differences between the model results and the experimental data are greater, so this model was not used to represent the evolution of ammonium in the effluent beyond the experimental data collected but was used to determine the minimum height of the column necessary to reach a certain set point value in the effluent.

The calculation of the minimum height of the bed volume can only be applied when the set point is below 15% of the Co. Maintaining the same criteria as was used to analyze the experimental data, the value of the effluent concentration was set at 0.5 mg NH_4-N/L. Table 9 shows the calibration of the parameters for the model in each test plus the value of the height required in the experiments.

Table 9. Fit parameters for the Bohart–Adams model and τ for the Yoon–Nelson model.

Test	k_{BA} (L mg^{-1} min^{-1})	q_{BA} (mg N-NH_4/g)	Z_0 (cm)	τ (min)
A1	0.940	1.713	5.03	1208
A2	0.870	1.224	3.89	1814
A3	0.328	1.750	3.50	4540
A4	0.454	2.468	9.02	777
A5	0.275	2.719	7.73	1672
A6	0.275	2.521	3.61	3493
A7	0.222	4.686	11.31	712
A8	0.125	4.538	10.65	1558
A9	0.064	5.456	8.60	2984

As expected, as the working flow rate was reduced, the contact time between the fluid and the active centers of the zeolites increased, thus less zeolite (lower column height) was needed. While at high flow values, the amount of ammonium exchanged per gram of zeolite and unit of time is lower, thus a higher column height is required to stay below the setpoint value. On the other hand, the higher the concentration of ammonium in the influent, the higher the column is necessary to ensure that the effluent meets the established requirements.

3.4.3. Yoon–Nelson

The experiment showed a good fit with the simulated values using the model proposed by Yoon and Nelson. Figure S8 shows for the A4 and A7 tests a strong correlation of $ln\left[\frac{C_t}{C_0-C_t}\right]$ vs. t, which was used to obtain the model parameters. Although this model also provides the evolution of ammonium in the column effluent, its main use is to determine the time at which 50% of the column (τ) is saturated. As this model can be considered a simplified version of the Thomas model, the values obtained for τ extracted by adjusting the Yoon–Nelson and Thomas models are quite similar, as can be seen in Figure S9 for Co = 27 and 54 mg NH_4-N/L.

The conclusions obtained from this model align with those reached by the other models. As the working flow rate increases, the time needed to reach the saturation state decreases (Table 9). This decrease is largely due to the fact that as the flow rate increases, the amount of ammonium treated per unit of time also increases proportionally, but it is observed how the value of τ decreases more sharply than the flow rate. For example, when the flow rate is reduced from 17.5 to 8.7 BV/h (Co = 54 mg NH_4-N/L), the time to reach 50% saturation decreases by 2.2 times. This slight variation in the reduction with respect

to the change of flow may be due to the fact that, as the flow rate increases, the zeolite decreases its maximum adsorption capacity.

On the other hand, it is observed that as the concentration of ammonium in the influent increased, the value of τ was reduced. This behavior was also reported by ref. [42], which worked with three different streams: contaminated river water (5 mg NH_4-N/L), rainwater runoff (8 mg NH_4-N/L), and domestic wastewater (25 mg NH_4-N/L). Its authors found that the more highly concentrated currents took less time to saturate (35 h for Co = 5 mg NH_4-N/L and 15 h for Co = 25 mg NH_4-N/L). This means that as the ammonium concentration increases, the maximum adsorption capacity does in fact also increase, but not in the same proportion as the increase in the influent ammonium concentration.

4. Conclusions

In this work, a natural zeolite was evaluated as an adsorbent material in a cation exchange process to retain ammonium from the permeate of AnMBR. The zeolite showed a good capacity to retain ammonium from urban wastewater AnMBR permeate, with values of qmax = 5.84 mg NH_4-N/g at 54 mg NH_4-N/L and Q = 4.4 BV/h. It has been observed that increasing the treatment flow rate reduces the working time but decreases the ammonium adsorption performance, so an economic analysis is necessary to determine the optimal flow rate. The results of the Thomas model confirm these conclusions and also indicate the importance of the effluent ammonium setpoint when the operational parameters are defined. NaOH can completely regenerate the zeolite with a Q of 8.8 BV/h and a concentration of 0.1 M. This concentration has been used to obtain the maximum efficiency in the use of the regenerant (0.221 mg NH_4-N/mg Na) and an ammonium concentration of 615 mg NH_4-N/L. Moreover, it has been possible to associate the presence of ammonium in the effluent during the adsorption phase and the end of the regeneration phase with the behavior of the effluent conductivity, indicating great potential for using this measure to optimize the duration of cation exchange cycles. The results achieved demonstrate that zeolites are a feasible technology to recover ammonium in the mainstream.

Supplementary Materials: The following supporting information can be downloaded at: https://www.mdpi.com/article/10.3390/w16192820/s1. Figure S1: This graph shows the relationship between conductivity and ammonium in the effluent during the regeneration phase for the first 7 BV treated. Figure S2: Calibration of the Thomas model, fitted linear regression obtained, and degree of adjustment (R2) calculated for (a) Q = 17.5 BV/h and Co = 27 mg NH_4-N/L and (b) Q = 17.5 BV/h and Co = 54 mg NH_4-N/L. Figure S3: Fitting experimental data from the A7 trial using the Thomas model. Figure S4: Relation of qth and Kth with the concentration of ammonium in the influent for a specific working flow rate (Q = 8.7 BV/h). Figure S5: Relation of qth and Kth with the working flow rate in the influent for a specific concentration of ammonium in the influent (C = 54 mg NH_4-N/L). Figure S6: Calibration of the Bohart–Adams model, fitted linear regression obtained, and degree of adjustment (R2) calculated for (a) Q = 17.5 BV/h and Co = 27 mg NH_4-N/L and (b) Q = 17.5 BV/h and Co = 54 mg NH_4-N/L. Figure S7: Adjustment of the experimental data obtained with Q = 17.5 BV/h and Co = 54 mg NH_4-N/L with the calibrated Bohart–Adams model. Figure S8: Calibration of the Yoon–Nelson model, fitted linear regression obtained, and degree of adjustment (R2) calculated for (a) Q = 17.5 BV/h and Co = 27 mg NH_4-N/L and (b) Q = 17.5 BV/h and Co = 54 mg NH_4-N/L. Figure S9: Time at which 50% of column saturation (τ) takes place for the Thomas and Yoon–Nelson model for (a) Co = 27 mg NH_4-N/L and (b) Co = 54 mg NH_4-N/L.

Author Contributions: J.G.: experimental work and writing; L.R.: experimental work; R.B.: experimental work supervision, writing, and article revision; S.H. and J.S.: writing and article revision. All authors have read and agreed to the published version of the manuscript.

Funding: This research was funded by the Ministry of Science and Innovation through the MEM4REC (CTM2017-86751-C2-2-R-AR) and RECREATE (PID2020-114315RB-C22) projects and by the Ministry of Universities (FPU17/00540).

Data Availability Statement: Data are contained within the article and Supplementary Materials.

Acknowledgments: The authors acknowledge the Ministry of Science and Innovation for supporting the projects "RECREATE" (PID2020-114315RB-C22) and "MEM4REC" (CTM2017-86751-C2-2-R-AR), under which this research is conducted, and the Ministry of Universities for funding the first author's research contract (FPU17/00540).

Conflicts of Interest: The authors declare no conflicts of interest. The funders had no role in the design of the study; in the collection, analyses, or interpretation of data; in the writing of the manuscript; or in the decision to publish the results.

References

1. World Economic Forum. *Global Risks Report 2019*; World Economic Forum: Cologny, Switzerland, 2019.
2. World Economic Forum. *Global Risks Report 2022*; World Economic Forum: Cologny, Switzerland, 2022.
3. Ferronato, N.; Rada, E.C.; Gorritty Portillo, M.A.; Cioca, L.I.; Ragazzi, M.; Torretta, V. Introduction of the circular economy within developing regions: A comparative analysis of advantages and opportunities for waste valorization. *J. Environ. Manag.* **2019**, *230*, 366–378. [CrossRef] [PubMed]
4. González-Camejo, J.; Jiménez-Benítez, A.; Ruano, M.V.; Robles, A.; Barat, R.; Ferrer, J. Optimising an outdoor membrane photobioreactor for tertiary sewage treatment. *J. Environ. Manag.* **2019**, *245*, 76–85. [CrossRef]
5. Robles, Á.; Capson-Tojo, G.; Gales, A.; Viruela, A.; Sialve, B.; Seco, A.; Steyer, J.P.; Ferrer, J. Performance of a membrane-coupled high-rate algal pond for urban wastewater treatment at demonstration scale. *Bioresour. Technol.* **2020**, *301*, 122672. [CrossRef] [PubMed]
6. Jiménez-Benítez, A.; Sanchís-Perucho, P.; Godifredo, J.; Serralta, J.; Barat, R.; Robles, A.; Seco, A. Ultrafiltration after primary settler to enhance organic carbon valorization: Energy, economic and environmental assessment. *J. Water Process Eng.* **2024**, *58*, 1048920. [CrossRef]
7. Jiménez-Benítez, A.; Ferrer, J.; Rogalla, F.; Vázquez, J.R.; Seco, A.; Robles, Á. Energy and environmental impact of an anaerobic membrane bioreactor (AnMBR) demonstration plant treating urban wastewater. In *Current Developments in Biotechnology and Bioengineering: Advanced Membrane Separation Processes for Sustainable Water and Wastewater Management—Case Studies and Sustainability Analysis*; Elsevier: Amsterdam, The Netherlands, 2020.
8. Sancho, I.; Lopez-Palau, S.; Arespacochaga, N.; Cortina, J.L. New concepts on carbon redirection in wastewater treatment plants: A review. *Sci. Total Environ.* **2019**, *647*, 1373–1384. [CrossRef] [PubMed]
9. Mezohegyi, G.; Bilad, M.R.; Vankelecom, I.F.J. Direct sewage up-concentration by submerged aerated and vibrated membranes. *Bioresour. Technol.* **2012**, *118*, 1–7. [CrossRef]
10. Fujioka, T.; Nghiem, L.D. Fouling control of a ceramic microfiltration membrane for direct sewer mining by backwashing with ozonated water. *Sep. Purif. Technol.* **2015**, *142*, 268–273. [CrossRef]
11. Gong, H.; Jin, Z.; Xu, H.; Wang, Q.; Zuo, J.; Wu, J.; Wang, K. Redesigning C and N mass flows for energy-neutral wastewater treatment by coagulation adsorption enhanced membrane (CAEM)-based pre-concentration process. *Chem. Eng. J.* **2018**, *342*, 304–309. [CrossRef]
12. Noriega-Hevia, G.; Serralta, J.; Seco, A.; Ferrer, J. Economic analysis of the scale-up and implantation of a hollow fibre membrane contactor plant for nitrogen recovery in a full-scale wastewater treatment plant. *Sep. Purif. Technol.* **2021**, *275*, 119128. [CrossRef]
13. Sheikh, M.; Lopez, J.; Reig, M.; Vecino, X.; Rezakazemi, M.; Valderrama, C.A.; Cortina, J.L. Ammonia recovery from municipal wastewater using hybrid NaOH closed-loop membrane contactor and ion exchange system. *Chem. Eng. J.* **2023**, *465*, 142859. [CrossRef]
14. Qin, Y.; Wang, K.; Xia, Q.; Yu, S.; Zhang, M.; An, Y.; Zhao, X.; Zhou, Z. Up-concentration of nitrogen from domestic wastewater: A sustainable strategy from removal to recovery. *Chem. Eng. J.* **2023**, *451*, 138789. [CrossRef]
15. Xi, J.; Zhou, Z.; Yuan, Y.; Xiao, K.; Qin, Y.; Wang, K.; An, Y.; Ye, J.; Wu, Z. Enhanced nutrient removal from stormwater runoff by a compact on-site treatment system. *Chemosphere* **2022**, *290*, 133314. [CrossRef] [PubMed]
16. Zhou, C.; An, Y.; Zhang, W.; Yang, D.; Tang, J.; Ye, J.; Zhou, Z. Inhibitory effects of Ca^{2+} on ammonium exchange by zeolite in the long-term exchange and NaClO–NaCl regeneration process. *Chemosphere* **2021**, *263*, 128216. [CrossRef]
17. Gong, H.; Wang, Z.; Zhang, X.; Jin, Z.; Wang, C.; Zhang, L.; Wang, K. Organics and nitrogen recovery from sewage via membrane-based pre-concentration combined with ion exchange process. *Chem. Eng. J.* **2017**, *311*, 13–19. [CrossRef]
18. Zhang, W.; Zhou, Z.; An, Y.; Du, S.; Ruan, D.; Zhao, C.; Ren, N.; Tian, X. Optimization for zeolite regeneration and nitrogen removal performance of a hypochlorite-chloride regenerant. *Chemosphere* **2017**, *178*, 565–572. [CrossRef]
19. Sancho, I.; Licon, E.; Valderrama, C.; de Arespacochaga, N.; López-Palau, S.; Cortina, J.L. Recovery of ammonia from domestic wastewater effluents as liquid fertilizers by integration of natural zeolites and hollow fibre membrane contactors. *Sci. Total Environ.* **2017**, *584–585*, 244–251. [CrossRef] [PubMed]
20. Guida, S.; Conzelmann, L.; Remy, C.; Vale, P.; Jefferson, B.; Soares, A. Resilience and life cycle assessment of ion exchange process for ammonium removal from municipal wastewater. *Sci. Total Environ.* **2021**, *783*, 146834. [CrossRef]
21. Wang, Y.; Liu, S.; Xu, Z.; Han, T.; Chuan, S.; Zhu, T. Ammonia removal from leachate solution using natural Chinese clinoptilolite. *J. Hazard. Mater.* **2006**, *136*, 735–740. [CrossRef] [PubMed]

22. Deng, Q.; Dhar, B.R.; Elbeshbishy, E.; Lee, H.S. Ammonium nitrogen removal from the permeates of anaerobic membrane bioreactors: Economic regeneration of exhausted zeolite. *Environ. Technol.* **2014**, *35*, 2008–2017. [CrossRef]
23. Damodara Kannan, A.; Parameswaran, P. Ammonia adsorption and recovery from swine wastewater permeate using naturally occurring clinoptilolite. *J. Water Process Eng.* **2021**, *43*, 102234. [CrossRef]
24. Mayor, Á.; Reig, M.; Vecino, X.; Cortina, J.L.; Valderrama, C. Advanced Hybrid System for Ammonium Valorization as Liquid Fertilizer from Treated Urban Wastewaters: Validation of Natural Zeolites Pretreatment and Liquid-Liquid Membrane Contactors at Pilot Plant Scale. *Membranes* **2023**, *13*, 580. [CrossRef] [PubMed]
25. Adam, M.R.; Othman, M.H.D.; Hubadillah, S.K.; Abd Aziz, M.H.; Jamalludin, M.R. Application of natural zeolite clinoptilolite for the removal of ammonia in wastewater. *Mater. Today Proc.* **2023**. [CrossRef]
26. Eberle, S.; Schmalz, V.; Börnick, H.; Stolte, S. Natural Zeolites for the Sorption of Ammonium: Breakthrough Curve Evaluation and Modeling. *Molecules* **2023**, *28*, 1614. [CrossRef]
27. Muscarella, S.M.; Laudicina, V.A.; Di Trapani, D.; Mannina, G. Recovering ammonium from real treated wastewater by zeolite packed columns: The effect of flow rate and particle diameter. *Sustain. Chem. Pharm.* **2024**, *41*, 101659. [CrossRef]
28. Godifredo, J.; Ferrer, J.; Seco, A.; Barat, R. Zeolites for Nitrogen Recovery from the Anaerobic Membrane Bioreactor Permeate: Zeolite Characterization. *Water* **2023**, *15*, 1007. [CrossRef]
29. Svobodová, E.; Tišler, Z.; Peroutková, K.; Strejcová, K.; Abrham, J.; Šimek, J. Adsorption of Heavy Metals on Alkali-Activated Zeolite Foams. *Materials* **2024**, *17*, 685. [CrossRef] [PubMed]
30. Lin, X.; Li, R.; Wen, Q.; Wu, J.; Fan, J.; Jin, X.; Qian, W.; Liu, D.; Chen, X.; Chen, Y.; et al. Experimental and Modeling Studies on the Sorption Breakthrough Behaviors of Butanol from Aqueous Solution in a Fixed-bed of KA-I Resin. *Biotechnol. Bioprocess Eng.* **2013**, *18*, 223–233. [CrossRef]
31. Singh, D.K.; Kumar, V.; Mohan, S.; Bano, D.; Hasan, S.H. Breakthrough curve modeling of graphene oxide aerogel packed fixed bed column for the removal of Cr(VI) from water. *J. Water Process Eng.* **2017**, *18*, 150–1580. [CrossRef]
32. Trgo, M.; Medvidović, N.V.; Perić, J. Application of mathematical empirical models to dynamic removal of lead on natural zeolite clinoptilolite in a fixed bed column. *IJCT* **2011**, *18*, 123–131.
33. Aksu, Z.; Gönen, F. Biosorption of phenol by immobilized activated sludge in a continuous packed bed: Prediction of breakthrough curves. *Process Biochem.* **2004**, *39*, 599–613. [CrossRef]
34. Paul Chen, J.; Chua, M.L.; Zhang, B. Effects of competitive ions, humic acid, and pH on removal of ammonium and phosphorous from the synthetic industrial effluent by ion exchange resins. *Waste Manag.* **2002**, *22*, 711–719. [CrossRef] [PubMed]
35. Malovanyy, A.; Sakalova, H.; Yatchyshyn, Y.; Plaza, E.; Malovanyy, M. Concentration of ammonium from municipal wastewater using ion exchange process. *Desalination* **2013**, *329*, 93–102. [CrossRef]
36. Sprynskyy, M.; Lebedynets, M.; Terzyk, A.P.; Kowalczyk, P.; Namieśnik, J.; Buszewski, B. Ammonium sorption from aqueous solutions by the natural zeolite Transcarpathian clinoptilolite studied under dynamic conditions. *J. Colloid Interface Sci.* **2005**, *284*, 408–415. [CrossRef] [PubMed]
37. Rahmani, A.R.; Mahvi, A.H.; Mesdaghinia, A.R.; Nasseri, S. Investigation of ammonia removal from polluted waters by Clinoptilolite zeolite. *Int. J. Environ. Sci. Technol.* **2004**, *1*, 125–133. [CrossRef]
38. Zheng, H.; Han, L.; Ma, H.; Zheng, Y.; Zhang, H.; Liu, D.; Liang, S. Adsorption characteristics of ammonium ion by zeolite 13X. *J. Hazard. Mater.* **2008**, *158*, 577–584. [CrossRef]
39. Ellersdorfer, M. The ion-exchanger-loop-stripping process: Ammonium recovery from sludge liquor using NaCl-treated clinoptilolite and simultaneous air stripping. *Water Sci. Technol.* **2018**, *77*, 695–705. [CrossRef]
40. Thornton, A.; Pearce, P.; Parsons, S.A. Ammonium removal from digested sludge liquors using ion exchange. *Water Res.* **2007**, *41*, 433–439. [CrossRef]
41. Canellas, J.; Soares, A.; Jefferson, B. Impact of Presence and Concentration of Ionic Species on Regeneration Efficacy of Zeolites for Ammonium Removal. *ChemRxiv* **2019**. [CrossRef]
42. Zhou, Z.; Wang, K.; Qiang, J.; Pang, H.; Yuan, Y.; An, Y.; Zhou, C.; Ye, J.; Wu, Z. Mainstream nitrogen separation and side-stream removal to reduce discharge and footprint of wastewater treatment plants. *Water Res.* **2021**, *188*, 116527. [CrossRef]
43. Stylianou, M.A.; Hadjiconstantinou, M.P.; Inglezakis, V.J.; Moustakas, K.G.; Loizidou, M.D. Use of natural clinoptilolite for the removal of lead, copper and zinc in fixed bed column. *J. Hazard. Mater.* **2007**, *143*, 575–581. [CrossRef]
44. Coury, L.; Ph, D. Conductance Measurements Part 1: Theory. *Current* **1999**, *3*, 91–96.
45. Du, Q.; Liu, S.; Cao, Z.; Wang, Y. Ammonia removal from aqueous solution using natural Chinese clinoptilolite. *Sep. Purif. Technol.* **2005**, *44*, 229–234. [CrossRef]
46. Rahmani, A.R.; Samadi, M.T.; Ehsani, H.R. Investigation **of** clinoptilolite natural zeolite regeneration by air stripping followed by ion exchange for removal of ammonium from aqueous solutions. *Iran. J. Environ. Heal. Sci. Eng.* **2009**, *6*, 167–172.
47. Mackinnon, I.D.R.; Barr, K.; Miller, E.; Hunter, S.; Pinel, T. Nutrient removal from wastewaters using high performance materials. *Water Sci. Technol.* **2003**, *47*, 101–107. [CrossRef]

Disclaimer/Publisher's Note: The statements, opinions and data contained in all publications are solely those of the individual author(s) and contributor(s) and not of MDPI and/or the editor(s). MDPI and/or the editor(s) disclaim responsibility for any injury to people or property resulting from any ideas, methods, instructions or products referred to in the content.